SLC24A5, a Putative Cation Exchanger, Affects Pigmentation in Zebrafish and Humans

Rebecca L. Lamason,[1]* Manzoor-Ali P.K. Mohideen,[1]† Jason R. Mest,[1] Andrew C. Wong,[1]‡ Heather L. Norton,[6] Michele C. Aros,[1] Michael J. Jurynec,[8] Xianyun Mao,[6] Vanessa R. Humphreville,[1]§ Jasper E. Humbert,[2,9] Soniya Sinha,[2] Jessica L. Moore,[1]‖ Pudur Jagadeeswaran,[10] Wei Zhao,[3] Gang Ning,[7] Izabela Makalowska,[7] Paul M. McKeigue,[11] David O'Donnell,[11] Rick Kittles,[12] Esteban J. Parra,[13] Nancy J. Mangini,[14] David J. Grunwald,[8] Mark D. Shriver,[6] Victor A. Canfield,[4] Keith C. Cheng[1,4,5]¶

Lighter variations of pigmentation in humans are associated with diminished number, size, and density of melanosomes, the pigmented organelles of melanocytes. Here we show that zebrafish *golden* mutants share these melanosomal changes and that *golden* encodes a putative cation exchanger slc24a5 (nckx5) that localizes to an intracellular membrane, likely the melanosome or its precursor. The human ortholog is highly similar in sequence and functional in zebrafish. The evolutionarily conserved ancestral allele of a human coding polymorphism predominates in African and East Asian populations. In contrast, the variant allele is nearly fixed in European populations, is associated with a substantial reduction in regional heterozygosity, and correlates with lighter skin pigmentation in admixed populations, suggesting a key role for the *SLC24A5* gene in human pigmentation.

Pigment color and pattern are important for camouflage and the communication of visual cues. In vertebrates, body coloration is a function of specialized pigment cells derived from the neural crest (*1*). The melanocytes of birds and mammals (homologous to melanophores in other vertebrates) produce the insoluble polymeric pigment melanin. Melanin plays an important role in the protection of DNA from ultraviolet radiation (*2*) and the enhancement of visual acuity by controlling light scatter (*3*). Melanin pigmentation abnormalities have been associated with inflammation and cancer, as well as visual, endocrine, auditory, and platelet defects (*4*).

Despite the cloning of many human albinism genes and the knowledge of over 100 genes that affect coat color in mice, the genetic origin of the striking variations in human skin color is one of the remaining puzzles in biology (*5*). Because the primary ultrastructural differences between melanocytes of dark-skinned Africans and lighter-skinned Europeans include changes in melanosome number, size, and density (*6*, *7*), we reasoned that animal models with similar differences may contribute to our understanding of human skin color. Here we present evidence that the human ortholog of a gene associated with a pigment mutation in zebrafish, *SLC24A5*, plays a role in human skin pigmentation.

The zebrafish *golden* phenotype. The study of pigmentation variants (*5*, *8*) has led to the identification of most of the known genes that affect pigmentation and has contributed to our understanding of basic genetic principles in peas, fruit flies, corn, mice, and other classical model systems. The first recessive mutation studied in zebrafish (*Danio rerio*), *golden* (gol^{b1}), causes hypopigmentation of skin melanophores (Fig. 1) and retinal pigment epithelium (Fig. 2) (*9*). Despite its common use for the calibration of germ-line mutagenesis (*10*), the *golden* gene remained unidentified.

The *golden* phenotype is characterized by delayed and reduced development of melanin pigmentation. At approximately 48 hours postfertilization (hpf), melanin pigmentation is evident in the melanophores and retinal pigment epithelium (RPE) of wild-type embryos (Fig. 2A) but is not apparent in *golden* embryos (Fig. 2B). By 72 hpf, *golden* melanophores and RPE begin to develop pigmentation (Fig. 2, F and G) that is lighter than that of wild type (Fig. 2, D and E). In adult zebrafish, the melanophore-rich dark stripes are considerably lighter in *golden* compared with wild-type animals (Fig. 1, A and B). In regions of the ventral stripes where melanophore density is low enough to distinguish individual cells, it is apparent that the melanophores of *golden* adults are less melanin-rich than those in wild-type fish (Fig. 1, A and B).

Transmission electron microscopy was used to determine the cellular basis of *golden* hypopigmentation in skin melanophores and RPE of ~55-hpf wild-type and *golden* zebrafish. Wild-type melanophores contained numerous, uniformly dense, round-to-oval melanosomes (Fig. 1, C and E). The melanophores of *golden* fish were thinner and contained fewer melanosomes (Fig. 1D). In addition, *golden* melanosomes were smaller, less electron-dense, and irregularly shaped (Fig. 1F). Comparable differences between wild-type and *golden* melanosomes were present in the RPE (fig. S1, A and B).

Dysmorphic melanosomes have also been reported in mouse models of Hermansky-Pudlak syndrome (HPS) (*11*, *12*). Because HPS is characterized by defects in platelet-dense granules and lysosomes as well as melano-

[1]Jake Gittlen Cancer Research Foundation, Department of Pathology; [2]Intercollege Graduate Degree Program in Genetics; [3]Department of Health Evaluation Sciences; [4]Department of Pharmacology; [5]Department of Biochemistry and Molecular Biology, The Pennsylvania State University College of Medicine, Hershey, PA 17033, USA. [6]Department of Anthropology, [7]The Huck Institutes of the Life Sciences, The Pennsylvania State University, University Park, PA 16802, USA. [8]Department of Human Genetics, University of Utah, Salt Lake City, UT 84112, USA. [9]Department of Genetics, Weis Center for Research, Danville, PA 17822, USA. [10]Department of Biological Sciences, University of North Texas, Denton, TX 76203, USA. [11]Conway Institute, University College Dublin, Belfield, Dublin 4, Ireland. [12]Department of Molecular Virology, Immunology and Medical Genetics, Ohio State University, Columbus, OH 43210, USA. [13]Department of Anthropology, University of Toronto at Mississauga, Mississauga, ON L5L 1C6, Canada. [14]Department of Anatomy and Cell Biology, Indiana University School of Medicine-Northwest, Gary, IN 46408, USA.

*Present address: The Graduate Program in Immunology, The Johns Hopkins University School of Medicine, Baltimore, MD 21205, USA.
†Present address: Health System Management Center, Case Western Reserve University, Cleveland, OH 44106, USA.
‡Present address: Department of Human Genetics, Emory University, Atlanta, GA 30322, USA.
§Present address: The Pennsylvania State University College of Medicine, H060, 500 University Drive, Hershey, PA 17033, USA.
‖Present address: Department of Biology, University of South Florida, Tampa, FL 33620, USA.
¶To whom correspondence should be addressed. E-mail: kcheng@psu.edu

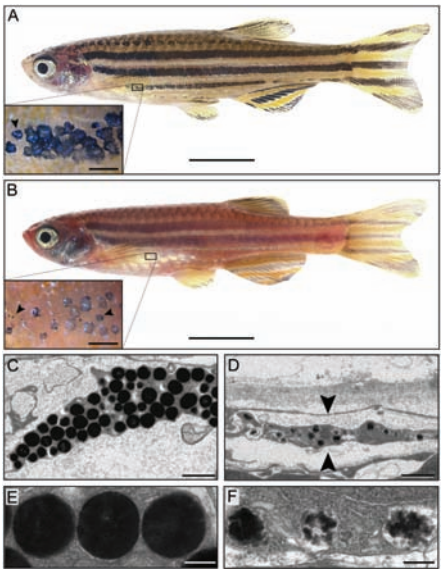

Fig. 1. Phenotype of *golden* zebrafish. Lateral views of adult wild-type (**A**) and *golden* (**B**) zebrafish. Insets show melanophores (arrowheads). Scale bars, 5 mm (inset, 0.5 mm). gol^{b1} mutants have melanophores that are, on average, smaller, more pale, and transparent. Transmission electron micrographs of skin melanophore from 55-hpf wild-type (**C** and **E**) and gol^{b1} (**D** and **F**) larvae. gol^{b1} skin melanophores (arrowheads show edges) are thinner and contain fewer melanosomes than do those of wild type. Melanosomes of gol^{b1} larvae are fewer in number, smaller, less-pigmented, and irregular compared with wild type. Scale bars in (C) and (D), 1000 nm; in (E) and (F), 200 nm.

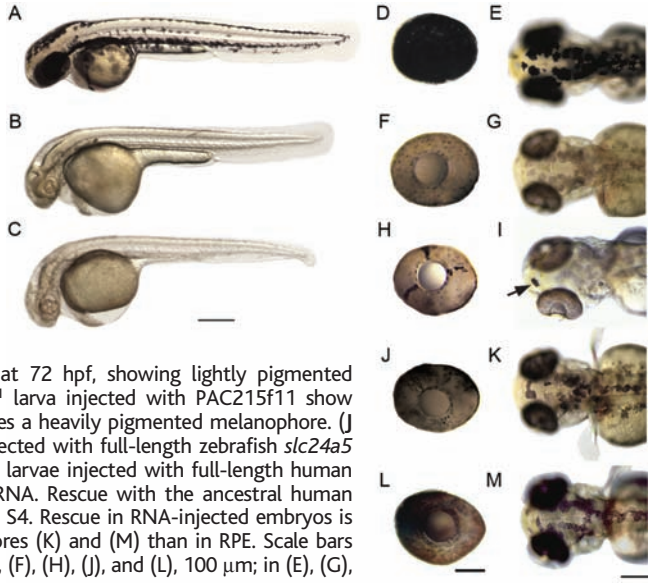

Fig. 2. Rescue and morpholino knockdown establish *slc24a5* as the *golden* gene. Lateral views of 48-hpf (**A**) wild-type and (**B**) gol^{b1} zebrafish larvae. (**C**) 48-hpf wild-type larva injected with morpholino targeted to the translational start site of *slc24a5* phenocopies the gol^{b1} mutation. Lateral view of eye (**D**) and dorsal view of head (**E**) of 72-hpf wild-type embryos. (**F** and **G**) gol^{b1} pigmentation pattern at 72 hpf, showing lightly pigmented cells. (**H** and **I**) 72 hpf gol^{b1} larva injected with PAC215f11 show mosaic rescue; arrow identifies a heavily pigmented melanophore. (**J** and **K**) 72-hpf gol^{b1} larva injected with full-length zebrafish *slc24a5* RNA. (**L** and **M**) 72-hpf gol^{b1} larvae injected with full-length human European (Thr^{111}) *SLC24A5* RNA. Rescue with the ancestral human allele (Ala^{111}) is shown in fig. S4. Rescue in RNA-injected embryos is more apparent in melanophores (K) and (M) than in RPE. Scale bars in [(A) to (C)], 300 μm; in (D), (F), (H), (J), and (L), 100 μm; in (E), (G), (I), (K), and (M), 200 μm.

somes, we examined whether the *golden* mutation also affects thrombocyte function in the zebrafish. A comparison of *golden* and wild-type larvae in a laser-induced arterial thrombosis assay (*13*) revealed no significant difference in clotting time (35 versus 30 s). The *golden* phenotype thus appears to be restricted to melanin pigment cells in zebrafish.

The zebrafish *golden* gene is *slc24a5/nckx5*. Similarities between zebrafish *golden* and light-skinned human melanosomes suggested that the positional cloning of *golden* might lead to the identification of a phylogenetically conserved class of genes that regulate melanosome morphogenesis. Positional cloning, morpholino knockdown, DNA and RNA rescue, and expression analysis were used to identify the gene underlying the *golden* phenotype. Linkage analysis of 1126 homozygous gol^{b1} embryos (representing 2252 meioses) revealed a single crossover between *golden* and microsatellite marker z13836 on chromosome 18. This map distance of 0.044 centimorgans (cM) [95% confidence interval (CI), 0.01 to 0.16 cM] corresponds to a physical distance of about 33 kilobases (kb) (using 1 cM = 740 kb) (*14*). Marker z9484 was also tightly linked to *golden* but informative in fewer individuals; no recombinants between z9484 and *golden* were identified in 468 embryos (95% CI, distance <0.32 cM). Polymerase chain reaction (PCR) analysis of a γ-radiation–induced deletion allele, gol^{b13} (*15*), showed a loss of markers z10264, z9404, z928, and z13836, but not z9484 (fig. S2A). Screening of a zebrafish genomic library (*16*) led to the identification of a clone (PAC215f11) containing both z13836 and z9484 within an ~85-kb insert. Microinjection of PAC215f11 into *golden* embryos produced mosaic rescue of wild-type pigmentation in embryonic melanophores and RPE (Fig. 2, H and I), indicating the presence of a functional *golden* gene within this clone.

Shotgun sequencing, contig assembly, and gene prediction revealed two partial and three complete genes within PAC215f11 (fig. S2B): the 3′ end of a thrombospondin-repeat–containing gene (*flj13710*), a putative potassium-dependent sodium/calcium exchanger (*slc24a5*), myelin expression factor 2 (*myef2*), a cortexin homolog (*ctxn2*), and the 5′ end of a sodium/potassium/chloride cotransporter gene (*slc12a1*). We screened each candidate gene using morpholino antisense oligonucleotides directed against either the initiation codon (*17*) or splice donor junctions (*18*). Only embryos injected with a morpholino targeted to *slc24a5* (either of two splice-junction morpholinos or one start codon morpholino) successfully phenocopied *golden* (Fig. 2C). In rescue experiments, injection of full-length, wild-type *slc24a5* transcript into homozygous gol^{b1} embryos led to the partial restoration of wild-type pigmentation in both melanophores and RPE (Fig. 2, J and K). Taken together, these results confirm the identity of *golden* as *slc24a5*.

To identify the mutation in the gol^{b1} allele, we compared complementary DNA (cDNA) and genomic sequence from wild-type and gol^{b1} embryos. A C→A nucleotide transversion that converts $Tyr^{\cdot 208}$ to a stop codon was found in gol^{b1} cDNA clones (GenBank accession number AY682554) and verified by sequencing gol^{b1} genomic DNA (fig. S3C). Conceptual translation of the mutant sequence predicts the truncation of the *golden* polypeptide to about 40% of its normal size, with loss of the central hydrophilic loop and the C-terminal cluster of potential transmembrane domains.

In wild-type embryos, the RNA expression pattern of *slc24a5* (Fig. 3A) resembled that of the melanin biosynthesis marker *dct* (Fig. 3B), consistent with expression of *slc24a5* in melanophores and RPE. In contrast, *slc24a5* expression was nearly undetectable in *golden* embryos (Fig. 3C), the expected result of nonsense-mediated mRNA decay (*19*). The extent of protein deletion associated with the gol^{b1} mutation, together with its low expression, suggests that gol^{b1} is a null mutation. The persistence of melanosome morphogenesis, despite likely absence of function, suggests that *golden* plays a modulatory rather than essential role in the formation of the melanosome. The pattern of *dct* expression seen in *golden* embryos (Fig. 3D) resembles that of wild-type embryos, indicating that the *golden* mutation does not affect the generation or migration of melanophores.

Conservation of *golden* gene structure and function in vertebrate evolution. Comparison of *golden* cDNA (accession number AY538713) to genomic (accession number AY581204) sequences shows that the wild-type gene contains nine exons (fig. S2C) encoding 513 amino acids (fig. S3A).

Fig. 3. Expression of *slc24a5* in zebrafish embryos and adult mouse tissues. The expression of *slc24a5* (**A**) and *dct* (**B**) in melanophores and RPE of a 24-hpf wild-type zebrafish larva show similar patterns. (**C**) gol^{b1} larvae lack detectable *slc24a5* expression. (**D**) *dct* expression in 24-hpf gol^{b1} larva is similar to that in wild type. Scale bar, 200 μm. (**E**) Quantitative RT-PCR analysis of *Slc24a5* expression in mouse tissues and B16 melanoma. Expression was normalized using the ratio between *Slc24a5* and the control transcript, RNA polymerase II (*Polr2e*).

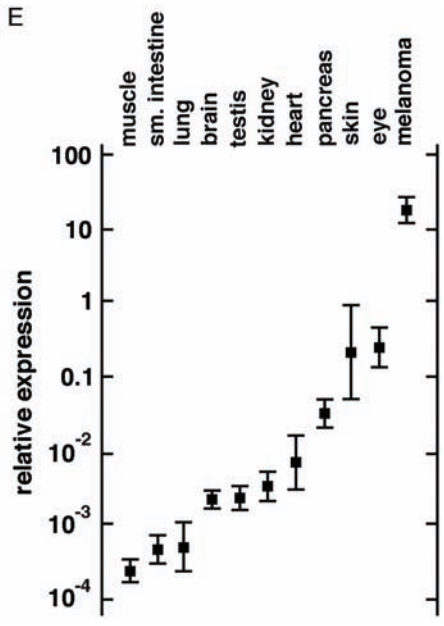

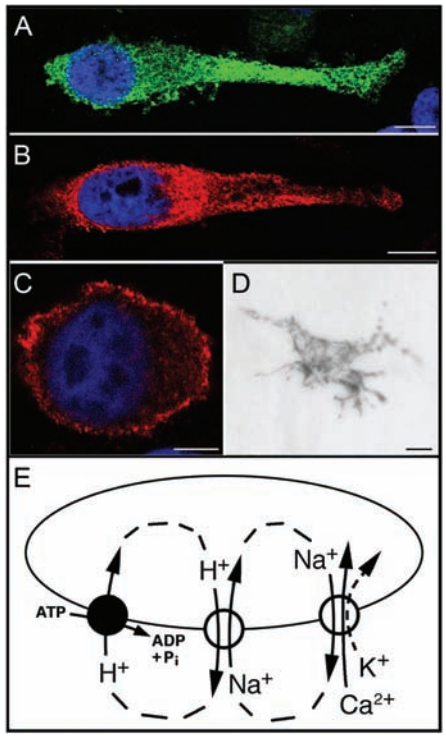

Fig. 4. Subcellular localization of slc24a5. Human MNT1 cells transfected with (**A**) GFP-tagged zebrafish slc24a5 (green) and (**B**) HA-tagged slc24a5 (red) clearly show intracellular expression. (**C**) HA-tagged D3 dopamine receptor localizes to the plasma membrane in MNT1 cells (red). 4′,6′-diamidino-2-phenylindole (DAPI) counterstain was used to visualize nuclei (blue). Scale bars in (A) and (B), 10 μm; in (C), 5 μm. (**D**) Rescue of dark pigmentation in a melanophore of a *golden* embryo by HA-tagged slc24a5. These dark cells appear in *golden* embryos injected with the HA-tagged construct, but not in mock-injected embryos. Scale bar, 10 μm. (**E**) Model for calcium accumulation in melanosomes. Protons are actively transported into the melanosome by the V-ATPase (left). The proton electrochemical potential gradient drives sodium uptake via the sodium (Na^+)/proton (H^+) exchanger (center). Sodium efflux is coupled to calcium uptake by the slc24a5 polypeptide (right). If potassium (dashed arrow) is cotransported with calcium, it must either accumulate within the melanosome or exit by means of additional transporters (not depicted). P_i, inorganic phosphate; ADP, adenosine diphosphate.

BLAST searches revealed that the protein is most similar to potassium-dependent sodium/calcium exchangers (encoded by the *NCKX* gene family), with highest similarity (68 to 69% amino acid identity) to murine *Slc24a5* (accession number BAC40800) and human *SLC24A5* (accession number NP_995322) (fig. S3B). The zebrafish *golden* gene shares less similarity with other human *NCKX* genes (35 to 41% identity to *SLC24A*1 to *SLC24A4*) or sodium/calcium exchanger (*NCX*) genes (26 to 29% identity to *SLC8A1* to *SLC8A3*). Shared intron/exon structure and gene order (*slc24a5*, *myef2*, *ctxn2*, and *slc12a5*) between fish and mammals further supports the conclusion that the zebrafish *golden* gene and *SLC24A5* are orthologs. The high sequence similarity among the orthologous sequences from fish and mammals (fig. S3A) suggested that function may also be conserved. The ability of human *SLC24A5* mRNA to rescue melanin pigmentation when injected into *golden* zebrafish embryos (Fig. 2, L and M, and fig. S4) demonstrated functional conservation of the mammalian and fish polypeptides across vertebrate evolution.

Tissue-specific expression of *Slc24a5*. Quantitative reverse transcriptase PCR (RT-PCR) was used to examine *Slc24a5* expression in normal mouse tissues and in the B16 melanoma cell line (Fig. 3E). *Slc24a5* expression varied 1000-fold between tissues, with concentrations in skin and eye at least 10-fold higher than in other tissues. The mouse melanoma showed ~100-fold greater expression of *Slc24a5* compared with normal skin and eye. These results suggest that mammalian *Slc24a5*, like zebrafish *golden*, appears to be highly expressed in melanin-producing cells.

Model for the role of SLC24A5 in pigmentation. SLC24A5 shares with other members of the protein family a potential hydrophobic signal sequence near the amino terminus and 11 hydrophobic segments, forming two groups of potential transmembrane segments separated by a central cytoplasmic domain. This structure is consistent with membrane localization, although the specific topology of these proteins remains controversial (*20*). Elucidation of the specific role of this exchanger in melanosome morphogenesis requires knowledge of its subcellular localization and transport properties. Although previously characterized members of the NCKX and NCX families have been shown to be plasma membrane proteins (*21*), the melanosomal phenotype of *golden* suggested the possibility that the slc24a5 protein resides in the melanosome membrane. To distinguish between these alternatives, confocal microscopy was used to localize green fluorescent protein (GFP)– and hemagglutinin (HA)-tagged derivatives of zebrafish slc24a5 in MNT1, a constitutively pigmented human melanoma cell line (*22*). Both slc24a5 fusion proteins displayed an intracellular pattern of localization (Fig. 4, A and B), which is distinct from that of a known plasma membrane control (Fig. 4C). The HA-tagged protein showed phenotypic rescue of the *golden* phenotype (Fig. 4D), indicating that tag addition did not abrogate its function. Taken together, these results indicate that the slc24a5 protein functions in intracellular, membrane-bound structures, consistent with melanosomes and/or their precursors.

Several observations suggest a model for the involvement of slc24a5 in organellar calcium uptake (Fig. 4E). First, the intracellular localization of the slc24a5 protein suggests that it affects organellar, rather than cytoplasmic, calcium concentrations, in contrast with other members of the NCX and NCKX families. Second, the accumulation of calcium in mammalian melanosomes appears to occur in a transmembrane pH gradient–dependent manner (*23*). Third, several subunits of the vacuolar proton adenosine triphosphatase (V-ATPase) and at least two intracellular sodium/proton exchangers have also been localized to melanosomes (*24*, *25*). In the model, active transport of pro-

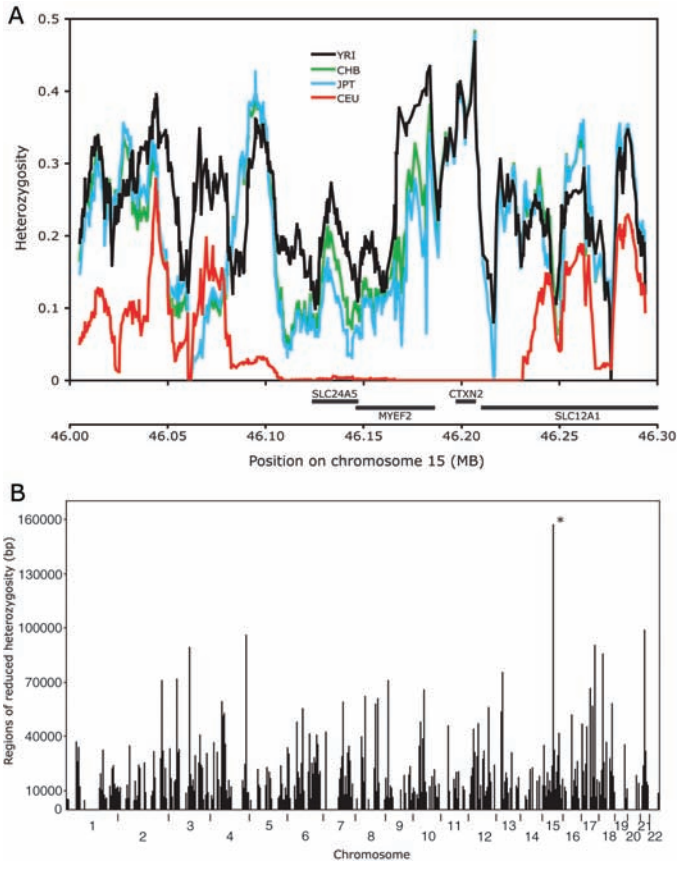

Fig. 5. Region of decreased heterozygosity in Europeans on chromosome 15 near *SLC24A5*. (**A**) Heterozygosity for four HapMap populations plotted as averages over 10-kb intervals. YRI, Yoruba from Ibadan, Nigeria (black); CHB, Han Chinese from Beijing (green); JPT, Japanese from Tokyo (light blue); CEU, CEPH (Foundation Jean Dausset–Centre d'Etude du Polymorphisme Humain) population of northern and western European ancestry from Utah (red). The data are from HapMap release 18 (phase II). (**B**) Distribution in genome of extended regions with low heterozygosity in the CEU sample. Only regions larger than 5 kb in which all SNPs have minor allele frequencies ≤0.05 and which contained at least one SNP with a population frequency difference between CEU and YRI of greater than 0.75 were plotted. Regions were divided at gaps between genotyped SNPs exceeding 10 kb. The data are from HapMap release 16c.1. An asterisk marks the region containing SLC24A5 within 15q21.

tons by the V-ATPase is coupled to slc24a5-mediated calcium transport via a sodium/proton exchanger. The melanosomal phenotype of the zebrafish *golden* mutant suggests that the calcium accumulation predicted by the model plays a role in melanosome morphogenesis and melanogenesis. The observations that processing of the melanosomal scaffolding protein pmel17 is mediated by a furin-like protease (*26*) and that furin activity is calcium-dependent (*27*) are consistent with this view. The role of pH in melanogenesis has been studied far more extensively than that of calcium, with alterations in pH affecting both the maturation of tyrosinase and its catalytic activity (*25*, *28*). The interdependence of proton and calcium gradients in the model may thus provide a second mechanism, in addition to calcium-dependent melanosome morphogenesis, by which the activity of slc24a5 might affect melanin pigmentation.

Role of *SLC24A5* in human pigmentation. To evaluate the potential impact of *SLC24A5* on the evolution of human skin pigmentation, we looked for polymorphisms within the gene. We noted that the G and A alleles of the single nucleotide polymorphism (SNP) rs1426654 encoded alanine or threonine, respectively, at amino acid 111 in the third exon of *SLC24A5*. This was the only coding SNP within SLC24A5 in the International Haplotype Map (HapMap) release 16c.1 (*29*). Sequence comparisons indicate the presence of alanine at the corresponding position in all other known members of the *SLC24* (*NCKX*) gene family (fig. S5). The SNP rs1426654 had been previously shown to rank second (after the FY null allele at the Duffy antigen locus) in a tabulation of 3011 ancestry-informative markers (*30*). The allele frequency for the Thr^{111} variant ranged from 98.7 to 100% among several European-American population samples, whereas the ancestral alanine allele (Ala^{111}) had a frequency of 93 to 100% in African, Indigenous American, and East Asian population samples (fig. S6) (*29*, *30*). The difference in allele frequencies between the European and African populations at rs1426654 ranks within the top 0.01% of SNP markers in the HapMap database (*29*), consistent with the possibility that this SNP has been a target of natural or sexual selection.

A striking reduction in heterozygosity near *SLC24A5* in the European HapMap sample (Fig. 5A) constitutes additional evidence for selection. The 150-kb region on chromosome 15 that includes *SLC24A5, MYEF2, CTNX2*, and part of *SLC12A1* has an average heterozygosity of only 0.0072 in the European sample, which is considerably lower than that of the non-European HapMap samples (0.175 to 0.226). This region, which contains several additional SNPs with high-frequency differences between populations, was the largest contiguous autosomal region of low heterozygosity in the European (CEU) population sample (Fig. 5B). This pattern of variation is consistent with the occurrence of a selective sweep in this genomic region in a population ancestral to Europeans. For comparison, diminished heterozygosity is seen in a 22-kb region encompassing the 3′ half of *MATP* (*SLC45A2*) in European samples, and more detailed analysis of this genomic region shows evidence for a selective sweep (*31*). However, the gene for agouti signaling protein (ASIP), which is known to be involved in pigmentation differences (*32*), shows no such evidence.

The availability of samples from two recently admixed populations, an African-American and an African-Caribbean population, allowed us to determine whether the rs1426654 polymorphism in *SLC24A5* correlates with skin pigmentation levels, as measured by reflectometry (*33*). Regression analysis using ancestry and *SLC24A5* genotype as independent variables revealed an impact of *SLC24A5* on skin pigmentation (Fig. 6). Despite considerable overlap in skin pigmentation between genotypic groups, regression lines for individuals with GG versus AG and GG versus AA genotypes were separated by about 7 and 9.5 melanin units, respectively (Fig. 6A). These differences are more evident in plots of skin pigmentation separated by genotype (Fig. 6B). *SLC24A5* genotype contributed an estimated 7.5, 9.5, or 11.2 melanin units to the differences in melanin pigmentation among African-Americans and African-Caribbeans in the dominant, unconstrained (additive effect plus dominance deviation), or additive models, respectively.

The computer program ADMIXMAP provides a test of gene effect that corrects for potential biases caused by uncertainty in the estimation of admixture from marker data (*34*). Score tests for association of melanin index with the *SLC24A5* polymorphism were significant in both African-American ($P = 3 \times 10^{-6}$) and African-Caribbean population subsamples ($P = 2 \times 10^{-4}$). The effect of *SLC24A5* on melanin index is between 7.6 and 11.4 melanin units (95% confidence limits). The data suggest that the skin-lightening effect of the A (Thr) allele is partially dominant to the G (Ala) allele. Based on the average pigmentation difference between European-Americans and African-Americans of about 30 melanin units (*33*),

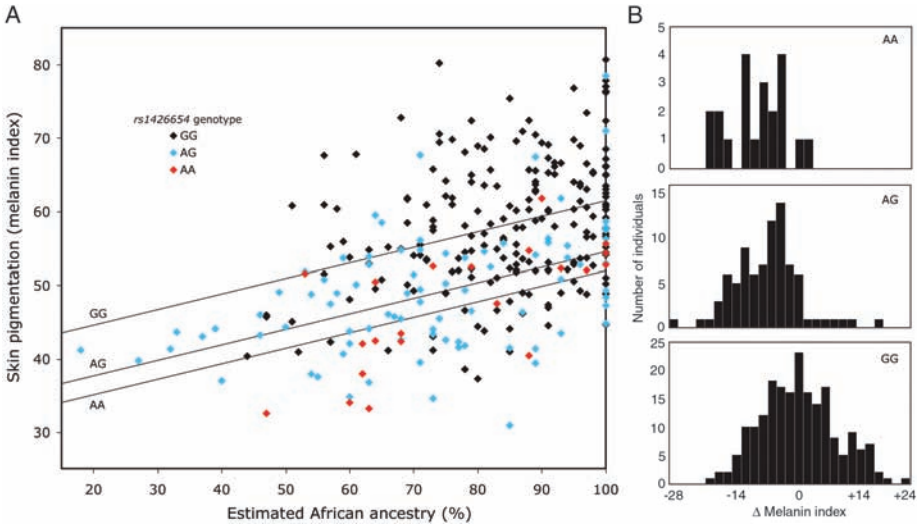

Fig. 6. Effect of *SLC24A5* genotype on pigmentation in admixed populations. (**A**) Variation of measured pigmentation with estimated ancestry and *SLC24A5* genotype. Each point represents a single individual; *SLC24A5* genotypes are indicated by color. Lines show regressions, constrained to have equal slopes, for each of the three genotypes. (**B**) Histograms showing the distribution of pigmentation after adjustment for ancestry for each genotype. Values shown are the difference between the measured melanin index and the calculated GG regression line ($y = 0.2113x + 30.91$). The corresponding uncorrected histograms are shown in fig. S7. Mean and SD (in parentheses) are given as follows: for GG, 0 (8.5), $n = 202$ individuals; for AG, –7.0 (7.4), $n = 85$; for AA, –9.6 (6.4), $n = 21$.

our results suggest that *SLC24A5* explains between 25 and 38% of the European-African difference in skin melanin index.

Relative contributions of *SLC24A5* and other genes to human pigment variation. Our estimates of the effect of *SLC24A5* on pigmentation are consistent with previous work indicating that multiple genes must be invoked to explain the skin pigmentation differences between Europeans and Africans (*5*, *35*). Significant effects of several previously known pigmentation genes have been demonstrated, including those of *MATP* (*36*), *ASIP* (*32*), *TYR* (*33*), and *OCA2* (*33*), but the magnitude of the contribution has been determined only for *ASIP*, which accounts for ≤4 melanin units (*32*). *MATP* may have a larger effect (*37*), but it can be concluded that much of the remaining difference in skin pigmentation remains to be explained.

Variation of skin, eye, and hair color in Europeans, in whom a haplotype containing the derived Thr^{111} allele predominates, indicates that other genes contribute to pigmentation within this population. For example, variants in *MC1R* have been linked to red hair and very light skin [reviewed in (*37*)], whereas *OCA2* or a gene closely linked to it is involved in eye color (*7*, *38*). The lightening caused by the derived allele of *SLC24A5* may be permissive for the effect of other genes on eye or hair color in Europeans.

Because Africans and East Asians share the ancestral Ala^{111} allele of rs1426654, this polymorphism cannot be responsible for the marked difference in skin pigmentation between these groups. Although we cannot rule out a contribution from other polymorphisms within this gene, the high heterozygosity in this region argues against a selective sweep in a population ancestral to East Asians. It will be interesting to determine whether the polymorphisms responsible for determining the lighter skin color of East Asians are unique to these populations or shared with Europeans.

The importance of model systems in human gene discovery. Our identification of the role of *SLC24A5* in human pigmentation began with the positional cloning of a mutation in zebrafish. Typically, the search for genes associated with specific phenotypes in humans results in multiple potential candidates. Our results suggest that distinguishing the functional genes from multiple candidates may require a combination of phylogenetic analysis, nonmammalian functional genomics, and human genetics. Such cross-disciplinary approaches thus appear to be an effective way to mine societal benefit from our investment in the human genome.

References and Notes

1. R. N. Kelsh, *Pigment Cell Res.* **17**, 26 (2004).
2. N. P. M. Smit *et al.*, *Photochem. Photobiol.* **74**, 424 (2001).
3. A. T. Hewitt, R. Adler, in *Retina*, S. J. Ryan, Ed. (The C. V. Mosby Company, St. Louis, MO, 1989), p. 57.
4. R. A. King, V. J. Hearing, D. J. Creel, W. S. Oetting, in *The Metabolic and Molecular Bases of Inherited Disease*, C. R. Scriver, A. L. Beaudet, W. S. Sly, D. Valle, Eds. (McGraw-Hill, St. Louis, MO, 2001), p. 5587.
5. G. S. Barsh, *PLoS Biol.* **1**, 19 (2003).
6. J. L. Bolognia, S. J. Orlow, in *Dermatology*, J. L. Bolognia, J. L. Jorizzo, R. P. Rapini, Eds. (Mosby, London, 2003), p. 935.
7. R. A. Sturm, T. N. Frudakis, *Trends Genet.* **20**, 327 (2004).
8. S. Fukamachi, A. Shimada, A. Shima, *Nat. Genet.* **28**, 381 (2001).
9. G. Streisinger, C. Walker, N. Dower, D. Knauber, F. Singer, *Nature* **291**, 293 (1981).
10. M. C. Mullins, M. Hammerschmidt, P. Haffter, C. Nusslein-Volhard, *Curr. Biol.* **4**, 189 (1994).
11. T. Nguyen *et al.*, *J. Invest. Dermatol.* **119**, 1156 (2002) .
12. T. Nguyen, M. Wei, *J. Invest. Dermatol.* **122**, 452 (2004).
13. M. Gregory, P. Jagadeeswaran, *Blood Cells Mol. Dis.* **28**, 418 (2002).
14. N. Shimoda *et al.*, *Genomics* **58**, 219 (1999).
15. C. Walker, G. Streisinger, *Genetics* **103**, 125 (1983).
16. C. T. Amemiya, L. I. Zon, *Genomics* **58**, 211 (1999).
17. A. Nasevicius, S. C. Ekker, *Nat. Genet.* **26**, 216 (2000).
18. B. W. Draper, P. A. Morcos, C. B. Kimmel, *Genesis* **30**, 154 (2001).
19. L. E. Maquat, *Curr. Biol.* **12**, R196 (2002).
20. K. D. Philipson, D. A. Nicoll, *Annu. Rev. Physiol.* **62**, 111 (2000).
21. X. Cai, J. Lytton, *Mol. Biol. Evol.* **21**, 1692 (2004).
22. M. Cuomo *et al.*, *J. Invest. Dermatol.* **96**, 446 (1991).
23. R. Salceda, G. Sanchez-Chavez, *Cell Calcium* **27**, 223 (2000).
24. V. Basrur *et al.*, *Proteome Res.* **2**, 69 (2003).
25. D. R. Smith, D. T. Spaulding, H. M. Glenn, B. B. Fuller, *Exp. Cell Res.* **298**, 521 (2004).
26. J. F. Berson *et al.*, *J. Cell Biol.* **161**, 521 (2003).
27. G. Thomas, *Nat. Rev. Mol. Cell Biol.* **3**, 53 (2002).
28. H. Watabe *et al.*, *J. Biol. Chem.* **279**, 7971 (2004).
29. The International HapMap Consortium, *Nature* **426**, 789 (2003); available at www.hapmap.org, release 16b, 31 May 2005.
30. M. W. Smith *et al.*, *Am. J. Hum. Genet.* **74**, 1001 (2004).
31. M. Soejima *et al.*, *Mol. Biol. Evol.*, doi: 10.1093/molbev/msj018 (2005).
32. C. Bonilla *et al.*, *Hum. Genet.* **116**, 402 (2005).
33. M. D. Shriver *et al.*, *Hum. Genet.* **112**, 386 (2003).
34. C. J. Hoggart *et al.*, *Am. J. Hum. Genet.* **72**, 1492 (2003).
35. G. A. Harrison, G. T. Owen, *Ann. Hum. Genet.* **28**, 27 (1964).
36. J. Graf, R. Hodgson, A. van Daal, *Hum. Mutat.* **25**, 278 (2005).
37. K. Makova, H. Norton, *Peptides* **26**, 1901 (2005).
38. T. Frudakis *et al.*, *Genetics* **165**, 2071 (2003).

39. We thank P. Hubley for excellent management of our zebrafish facility; B. Blasiole, W. Boehmler, A. Sidor, and J. Gershenson for experimental assistance; R. Levenson, B. Kennedy, G. Chase, J. Carlson, and E. Puffenberger for helpful discussions; L. Rush for help on the cover design; and V. Hearing and M. Marks for MNT1 cells. Supported by funding from the Jake Gittlen Memorial Golf Tournament (K.C.), NSF (grant MCB9604923 to K.C.), NIH (grants CA73935, HD40179, and RR017441 to K.C.; HD37572 to D.G.; HG002154 to M.S.; EY11308 to N.M.; and HL077910 to P.J.), the Pennsylvania Tobacco Settlement Fund (K.C.), and the Natural Sciences and Engineering Research Council of Canada (E.P.). This work is dedicated to the open, trusting, and generous atmosphere fostered by the late George Streisinger.

Supporting Online Material
www.sciencemag.org/cgi/content/full/310/5755/1782/DC1
Materials and Methods
Figs. S1 to S7
References

17 June 2005; accepted 15 November 2005
10.1126/science.1116238

Supporting Online Material for

SLC24A5, a Putative Cation Exchanger, Affects Pigmentation in Zebrafish and Humans

Rebecca L. Lamason, Manzoor-Ali P.K. Mohideen, Jason R. Mest, Andrew C. Wong, Heather L. Norton, Michele C. Aros, Michael J. Jurynec, Xianyun Mao, Vanessa R. Humphreville, Jasper E. Humbert, Soniya Sinha, Jessica L. Moore, Pudur Jagadeeswaran, Wei Zhao, Gang Ning, Izabela Makalowska, Paul M. McKeigue, David O'Donnell, Rick Kittles, Esteban J. Parra, Nancy J. Mangini, David J. Grunwald, Mark D. Shriver, Victor A. Canfield, Keith C. Cheng*

*To whom correspondence should be addressed. E-mail: kcheng@psu.edu

Published 16 December 2005, *Science* **310**, 1782 (2005)
DOI: 10.1126/science.1116238

This PDF file includes:

Supporting Online Materials

Experimental Procedures

Fish Culture

Zebrafish were maintained as described (*S1*). Wild-type zebrafish were obtained from Lyles Tropical Fish (Ruskin, FL); *gol*^{b1}, WIK and AB lines were obtained from the Zebrafish International Resource Center (Eugene, OR).

Histological and in situ hybridization analyses

Tissue sections from adult and larval zebrafish skin and retina were prepared as previously described (*S2, S3*). Thin sections were examined with a JEOL 1200 EX transmission electron microscope. Whole mount *in situ* hybridization was performed (*S4*) using a previously described *dct* (*trp2*) probe (*S5*) or a *golden* probe corresponding to a 650 bp fragment of the *slc24a5* cDNA (nt 580-1229). Photography was done in the Penn State Zebrafish Functional Genomics Core Facility.

Genetic Mapping and Genomics

The *gol*^{b1} locus was mapped to LG 18 by S. Johnson and J. Postlethwait (personal communications). The *gol*^{b1} genetic interval was refined by genotyping 1126 *golden* embryos recovered from crosses between *gol*^{b1}*/AB or gol*^{b1}*/WIK* heterozygotes for linked markers (*S6, S7*). These primer pairs were also used for detection of markers in a deletion strain and to identify clones from a genomic library (*16*). PAC215f11 included *gol*-linked markers and rescued the *golden* phenotype and so was subjected to shotgun DNA sequence analysis. As PAC215f11 contained a high density of repeat elements that prevented construction of a high coverage library generated from randomly sheared PAC DNA, two alternate libraries were constructed for sequencing: a random transposon insertion library (GPS-1 Genome Priming

System, NEB) and a library consisting of fragments generated by partial *Hpy*CH4V digestion. Sequences were error-checked and assembled into contigs using the Phred/Phrap programs (*S8, S9*). Gene prediction, similarity searches, and annotation employed GeneMachine (*S10*), BLAST (*S11*), and GCG programs (*S12*).

To confirm the *gol*^{b1} mutation, genomic DNA was isolated from 4 dpf larvae (DNeasy Tissue Kit, Qiagen), a ~150 bp segment of DNA containing the nonsense mutation in *gol*^{b1} was amplified using primers StopF1 (5'-CTGGCCGTTGTTCAGAGATTGTG-3') and StopR2 (5'-CAGAGAATAAAGTGAGGAGTGATGG-3'), and the PCR products were sequenced. Sequencing was performed in the Sequencing Core of the Jake Gittlen Cancer Research Foundation and the Penn State College of Medicine Macromolecular Core Facility.

RNA isolation and cDNA cloning

RNAs were isolated using either TRIzol Reagent (Invitrogen) or the RNeasy and Qiashredder kits (Qiagen). RNA isolated from 31-36 hpf zebrafish larvae pre-scored for *golden* phenotype was subjected to 5'- and 3'-RACE using GeneRacer (Invitrogen). The gene specific primers for 5'RACE were: 5Race3 (5'-GCGAGGTTTCAGACACCAGCAGCA-3') and 5Race4 (nested) (5'-CTGAACAACGGCCAGCAGCTCAGA-3'); and for 3'RACE were 3Race3 (5'-TCCCGGACACAGTGATGGGAATGA-3') and 3Race4 (nested) (5'-AGTATCCCCGACACCGTGGCCAGT-3'). The full-length cDNA sequence was 2003 nt, with the coding region spanning nt 61 to 1602 (accession AY538713).

Knockdown and Rescue Experiments

For morpholino knockdown and DNA or RNA rescue experiments, approx. 1 nl solution containing 0.05% Phenol Red was injected into 1-4-cell embryos. The following morpholino oligonucleotides (Gene Tools) were used (sequence complementary to the intron is underlined

for splice-junction morpholinos): *ctxn2*, 5'-ATGTTCCCGCTCCAGCCCCAGCATC-3'; *myef2*, 5'-TGTGAGACTCACGTTGGCCACAAAG-3' and 5'-CTGCTCGAAGGTCACCGTCCCCATC-3'; *flj13710*, 5'-AGCTGCTGCTCACCTGAGCGCTCCA-3' and 5'-TTTTGATAGCTGTACCTGGCTCCTG-3'; *slc24a5*, 5'-TAGTCACGCACTGCAGAGGACAGCA-3', 5'-AGGCTCACCAGTAAACTCTGTTATC-3' and 5'-GCTGGAGAAACACGTCTGTCCTCAT-3'. Morpholinos were prepared in 1x Danieau buffer (*S1*). PAC rescue was performed as previously described (*S13*) using 0.075 ng of DNA. For human rescue, experiments, SLC24A5 cDNA was amplified using RNA from human RPE as template. The resultant cDNA contained Thr-111. An Ala-111 allele with only the same single nucleotide change associated with the African allele in human populations was produced from this clone using PCR mutagenesis. Capped RNA transcripts were produced by in vitro transcription (mMESSAGEmMACHINE kit, Ambion) of template cDNAs cloned in the pT3TS vector (*S14*) or CS2+ (*S15*) vectors. Zebrafish slc24a5 was expressed from pT3TS and N-terminal HA-tagged zebrafish slc24a5 was expressed from CS2+-HA. Human SLC24A5(Thr111) was expressed from pT3TS and SLC24A5(Ala111) was expressed from CS2+. SLC24A5(Ala111) was generated by in vitro mutagenesis of the Thr111 allele. Capped RNA transcripts were produced by in vitro transcription (mMESSAGEmMACHINE kit, Ambion). Rescue experiments were performed by injection of either 0.0625 – 0.1 ng/nl RNA or 0.025 ng/nl DNA into *golden* 1-cell zygotes. RNA rescues were performed using 0.0625 ng/nl RNA.

Quantitative PCR

B16-F1 cells were obtained from ATCC. Mouse tissue and B16 RNA was reverse transcribed using the SuperScript II First Strand cDNA Synthesis Kit (Invitrogen). Quantitative

PCR was performed on mouse tissue and B16 cDNA using the Brilliant SYBR Green QPCR Core Reagent Kit (Stratagene) according to the manufacturer's protocol using the MX4000 Multiplex Quantitative PCR System (Stratagene). Experimental primers mu5f1 (5' – GGGATCCCAGACACAGTGAT – 3') and mu5r1 (5' – GGGAAGACCTAGGCATAGCA – 3') amplified a ~162 bp segment of mu *SLC24A5*. Control primers muPolr2eF2 (5' – CACGGTACTTTGGGATCAAG – 3') and muPolr2eR2 (5' – TGTGGGTTCCTCTTCATTGT – 3') amplified ~204bp segment of murine *RNA polymerase II*. Amplification efficiency as estimated by analysis of samples at two dilutions was used to extrapolate to initial concentrations.

Subcellular Localization

GFP was fused to the C-terminus of zebrafish *slc24a5* in vector pEGFP-N1 (Clontech). A triple HA-tag fusion at the C-terminus of zebrafish *slc24a5* was inserted into vector pCDNA3.1 (Invitrogen). The positive control for plasma membrane expression was a monkey dopamine D3 receptor cDNA with an N-terminal HA tag, in the vector pCB6 (*S16*). DNA constructs were transfected into MNT1 cells using Effectene reagent (Qiagen) according to the manufacturer's protocols. The HA tag was visualized using the monoclonal anti-HA antibody 16B12 at 1:500 (Covance) and Cy3-conjugated goat anti-mouse antibody at 1:800 (Jackson Immunoresearch) as previously described (*S17*). Confocal images were obtained using a Leica TCS SP2 AOBS microscope in the Microscopy Imaging Core Facility of the Penn State College of Medicine.

Human population genetics

Frequency differences between the CEU and YRI populations were calculated for each autosomal SNP in HapMap release 16c.1 (*29*). rs1426654 ranked 30-37 (indeterminate due to

ties) out of 977,676 SNPs in this comparison. Similar results are observed in whole-genome comparisons of F_{ST} calculated as previously described (*S18*) or locus-specific branch length (*S19*).

Statistical methods: testing associations with genotype

To investigate associations with genotype, we studied samples of 105 African Caribbean and 203 African American individuals whose skin melanin content (M index) had been measured on the inner arm with a narrow-band reflectometer (*S20*). Accordingly, these individuals had been typed at 33 ancestry-informative marker loci as described previously, allowing 3-way genetic admixture between west African, European, and Native American ancestry to be modeled (*33*). This modeling of genetic admixture is necessary in order to control for hidden population stratification when testing associations of skin pigmentation with genotype (*S21*). We used the ADMIXMAP program (*S22, 34; http://www.ucd.ie/genepi/software.html*) to fit a linear regression of M index on sex and individual admixture proportions inferred from the marker and trait data. Score tests for association with *SLC24A5* genotype were calculated by averaging over the posterior distribution of missing-data as described previously. This test allows for uncertainty in estimation of individual admixture proportions from marker data. The effect of this locus was examined also by including terms for additive effect (average effect of one extra copy of allele A) and dominance deviation (heterozygote mean minus mean of both homozygotes) in the regression model.

The African-Caribbean, but not the African-American population, shows significant deviations from Hardy-Weinberg equilibrium ($p = 0.02$). When admixture in the African-Caribbean population was modeled with ADMIXMAP, the observed and expected frequencies of heterozygotes did not differ significantly, consistent with hidden stratification in this population

(*S21*) as an explanation for the deficit of heterozygotes in the crude analysis.

SOM References

S1. M. Westerfield, *The Zebrafish Book: A guide to the Laboratory Use of Zebrafish (Danio rerio)* (University of Oregon Press, Eugene, 1995).

S2. R. Chen *et al*., *J. Clin. Invest.* **108**, 1151 (2001).

S3. Y. H. Datta *et al*., *Thromb. Haemost.* **89**, 1031 (2003).

S4. T. Jowett, *Methods Cell Biol.* **59**, 63 (1999).

S5. R. N. Kelsh, B. Schmid, J. S. Eisen, *Development* **225**, 277 (2000).

S6. E. E. Gestl, E. J. Kauffman, J. L. Moore, K. C. Cheng, *J. Hered.* **88**, 76 (1997).

S7. M. A. Mohideen, J. L Moore, K. C. Cheng, *Genomics* **67**, 102 (2000).

S8. B. Ewing, L. Hillier, M. C. Wendl, P. Green, *Genome Res*. **8**, 175 (1998).

S9. B. Ewing and P. Green, *Genome Res*. **8**, 186 (1998).

S10. I. Makalowska, J. F. Ryan, A. D. Baxevanis, *Bioinformatics* **17**, 843 (2001).

S11. S. F. Altschul, W. Gish, W. Miller, E. W. Myers, D. J. Lipman, *J. Mol. Biol*. **215**, 403 (1990).

S12. J. Devereux, P. Haeberli, O. Smithies, *Nucleic Acids Res*. **12**, 387 (1984).

S13. Y. L. Yan, W. S. Talbot, E. S. Egan, J. H. Postlethwait, *Genomics* **50**, 287 (1998).

S14. T. N. Hyatt, S.C. Ekker, in *The Zebrafish: Biology*, H. W. Detrich III, M. Westerfield, L. I. Zon, Eds. (Academic Press, San Diego, 1999), pp. 117-126.

S15. D. L. Turner, H. Weintraub, *Genes Dev*. **8**, 1434 (1994).

S16. C. B. Brewer, M. G. Roth *J. Cell Biol*. **114**, 413 (1991).

S17. V. A. Canfield, R. Levenson, *Biochemistry*, **32**, 13782 (1993).

S18. J. M. Akey, G. Zhang, K. Zhang, L. Jin, M. D. Shriver, *Genome Res*. **12**, 1805 (2002).

S19. M. D. Shriver *et al.*, *Human Genomics*, **1**, 274 (2004).

S20. M. D. Shriver, E. J. Parra, *Am. J. Phys. Anthropol*. **112**, 17 (2000).

S21. E. J. Parra, R. A. Kittles, M. D. Shriver, *Nat. Genet*. **36**, S54 (2004).

S22. C. J. Hoggart, M. D. Shriver, R. A. Kittles, D. G. Clayton, P. M. McKeigue, *Am. J. Hum. Genet*. **74**, 965 (2004).

SOM Figures & Legends:

Fig. S1.

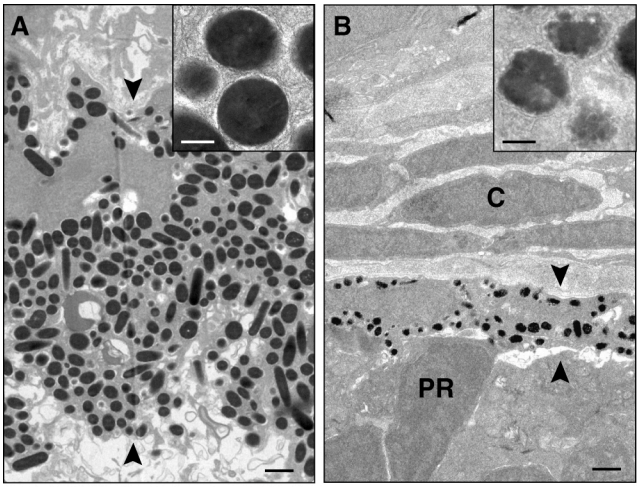

The *golden* phenotype in retinal pigment epithelium. (**A**) Wild-type RPE cells (72 hpf) are large and contain numerous large, round melanosomes. (**B**) The RPE cells of *gol*^{b1} are much smaller and contain fewer melanosomes. These melanosomes are smaller and less densely pigmented. Arrowheads indicate boundaries of the RPE. PR, photoreceptor cell; C, choroid. Scale bars: 1000nm (150nm inset).

Fig. S2.

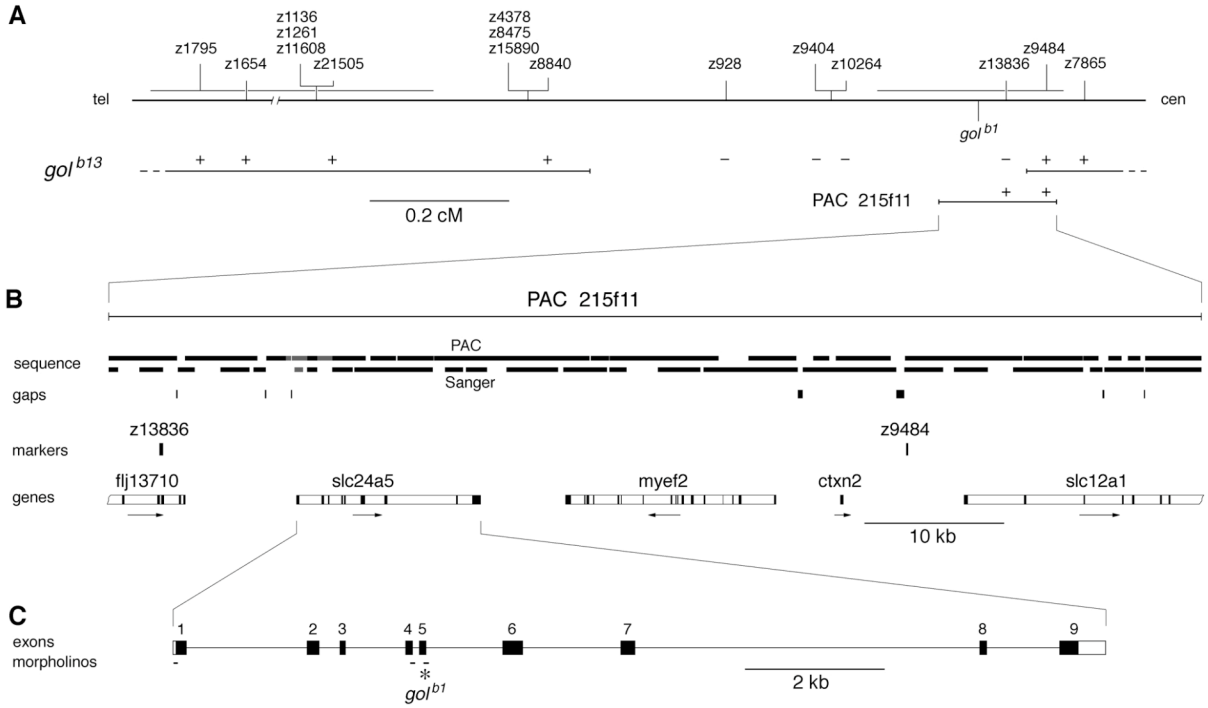

Positional cloning of the *golden* gene (**A**) Genomic map of the portion of LG 18 including *golden*. Genotyping did not order z1795 and z9484 with respect to adjacent markers; horizontal lines indicate the range of potential marker positions. Markers from z928 to z13836 are deleted in gol^{b13}. (**B**) Genomic sequence of PAC215f11 determined from assembly of shotgun and transposon-insertion-based sequences from PAC215f11 (above) and by the Sanger Center (below). Remaining gaps in the compiled sequence are indicated. The PAC contains portions of genes *flj13710* and *slc12a1* and all of *slc24a5*, *myef2*, and *ctxn2*. Arrows indicate the direction of transcription. (**C**) The *golden/slc24a5* gene has nine exons. Coding regions are shown as closed boxes, and non-coding regions as open boxes. The asterisk indicates the position of the gol^{b1} mutation. Positions of the three tested morpholinos are indicated by dashes.

Fig. S3.

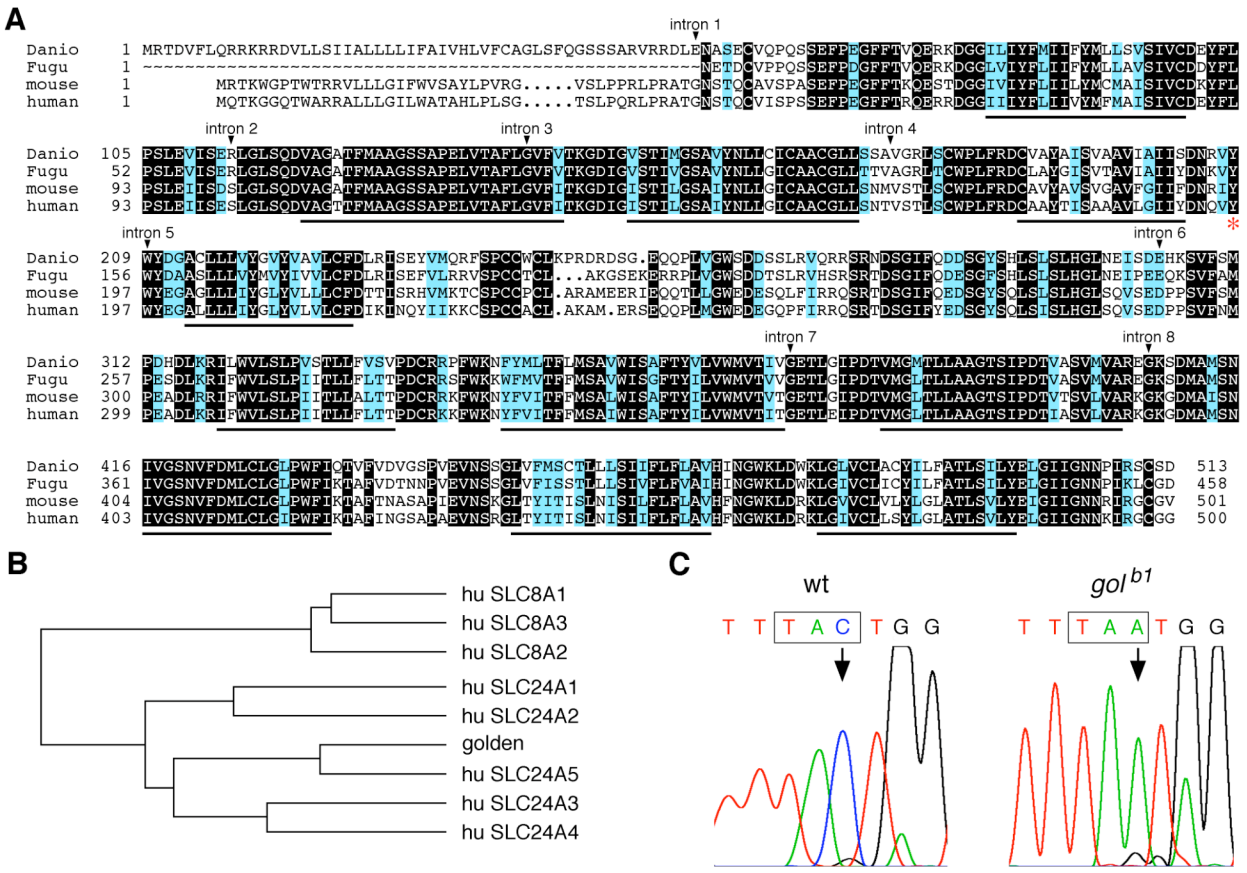

Sequence analysis of the *golden* gene. (**A**) Protein comparison between zebrafish *slc24a5* and the orthologous polypeptides of human, mouse, and *Fugu*. Identical sequences are black, and conserved regions blue. Potential transmembrane segments are underlined, and intron positions are indicated above. The position of the *gol*^{b1} nonsense mutation is indicated by a red asterisk. Sources of sequences: human SLC8A1 (NP_066920), SLC8A2 (Q9UPR5), SLC8A3 (NP_150287), SLC24A1 (NP_004718), SLC24A2 (NP_065077), SLC24A3 (NP_065740), SLC24A4 (NP_705932), SLC24A5 (NP_995322); mouse (BAC40800), *Fugu* (BK004894/CAAB01000235), zebrafish *golden/slc24a5* (AY538713, this paper). (**B**) Similarity dendrogram of zebrafish *slc24a5* and human sodium, calcium exchanger polypeptides produced using the PILEUP program (S12). (**C**) Sequence traces of genomic DNA show C→A mutation in the 5th exon (codon 208, boxed) of *gol*^{b1}.

Fig. S4.

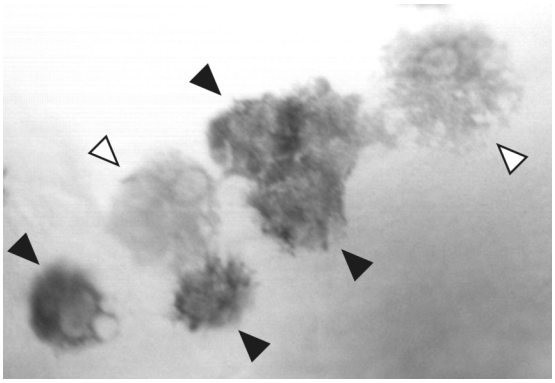

Rescue of the zebrafish *golden* phenotype by human SLC24A5(Ala111). Neighboring darkly pigmented (*SLC24A5*$^{+}$, filled arrowheads) and lightly pigmented *golden* (*gol*) cells (open arrowheads) in 60 hpf *golden* embryos following injection of *golden* zygotes with a DNA expression plasmid containing human *SLC24A5*(*Ala111*).

Fig. S5.

Alignment of SLC24A5 near rs1426654. Partial sequences of SLC24A5 orthologues from various vertebrate species are shown in alignment. The position of rs1426654 (aa 111) is marked by an asterisk, and the amino acids encoded by the G and A alleles are shown in red. Residues that are conserved in all SLC24A5 sequences and all SLC24 family sequences (vertebrate and invertebrate) are shown at the bottom. Accession numbers for sequences: Zebrafish, this paper; medaka, BJ713544; Fugu rubripes, CAAB01000235; three-spined stickleback, DN686371; Xenopus tropicalis, DN099900; chicken, XP_413812; dog, XP_851849; cow, Bt10_WGA1838_2; rabbit, DN890784; mouse, AAH94232; rat, XP_230584; chimpanzee, XP_510380; human, NP_995322.

Fig. S6.

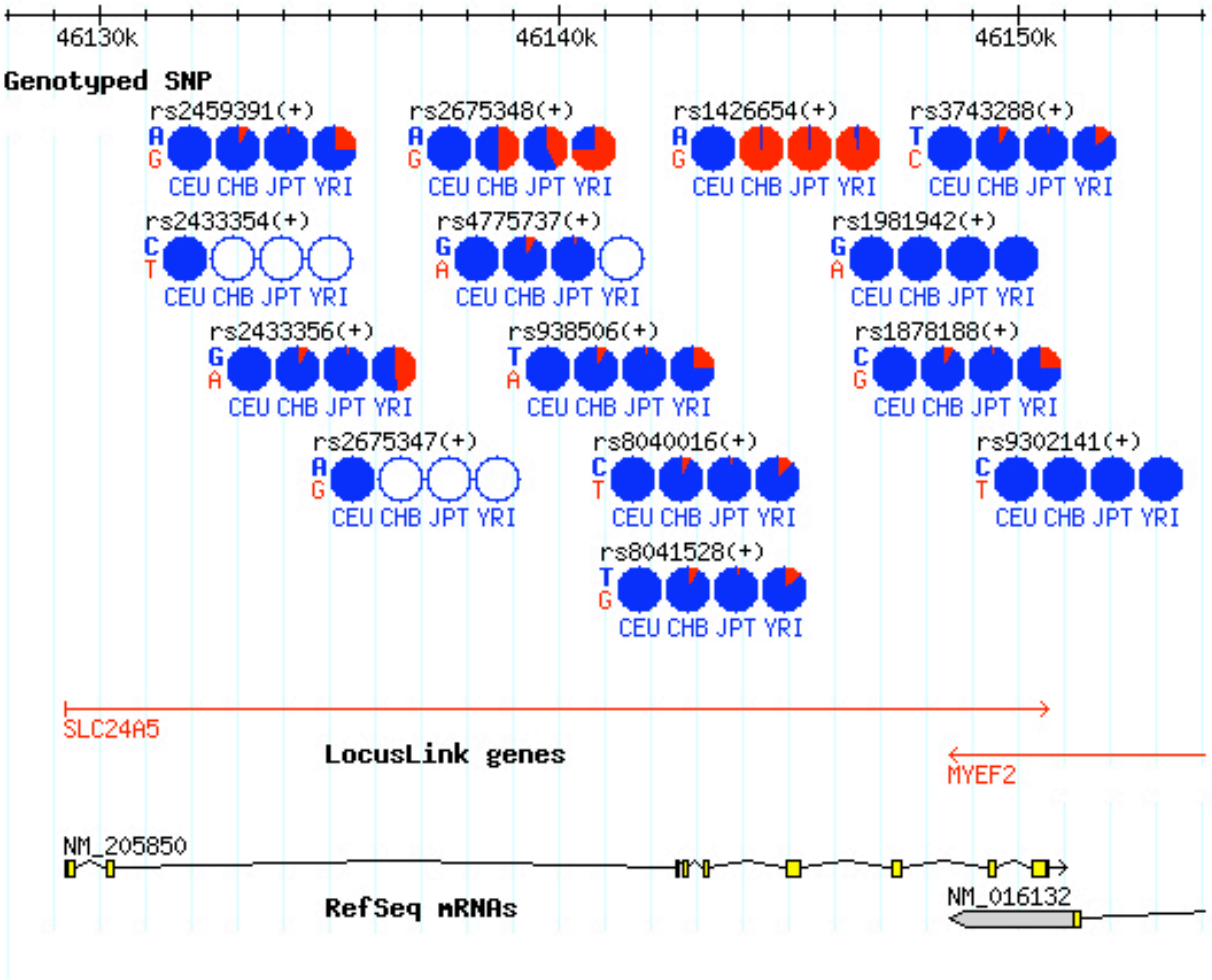

SNP allele frequencies in *SLC24A5*. Each group of four circles represents the distribution of alleles in the CEPH population in Utah (Northern/Western European; CEU), Han Chinese in Beijing (CHB), Japanese in Tokyo (JPT) and Yoruban tribe in West Africa (YRI); each circle is a pie-chart of allele frequencies whose colors correspond to the individual base of corresponding color code, designated for each group of four circles. Open circles indicate lack of genotypic data. Note the result for rs1426654, for which the *G* allele (red), which corresponds with the ancestral Alanine a position 111, predominates in the CHG, JPT and YRI populations, and for which CEU population is 100% the derived allele, *A* (blue), which corresponds to the *Thr* allele. The extent of the gene and positions of the exons are indicated at the bottom. Adapted from www.HapMap.org.

Fig. S7.

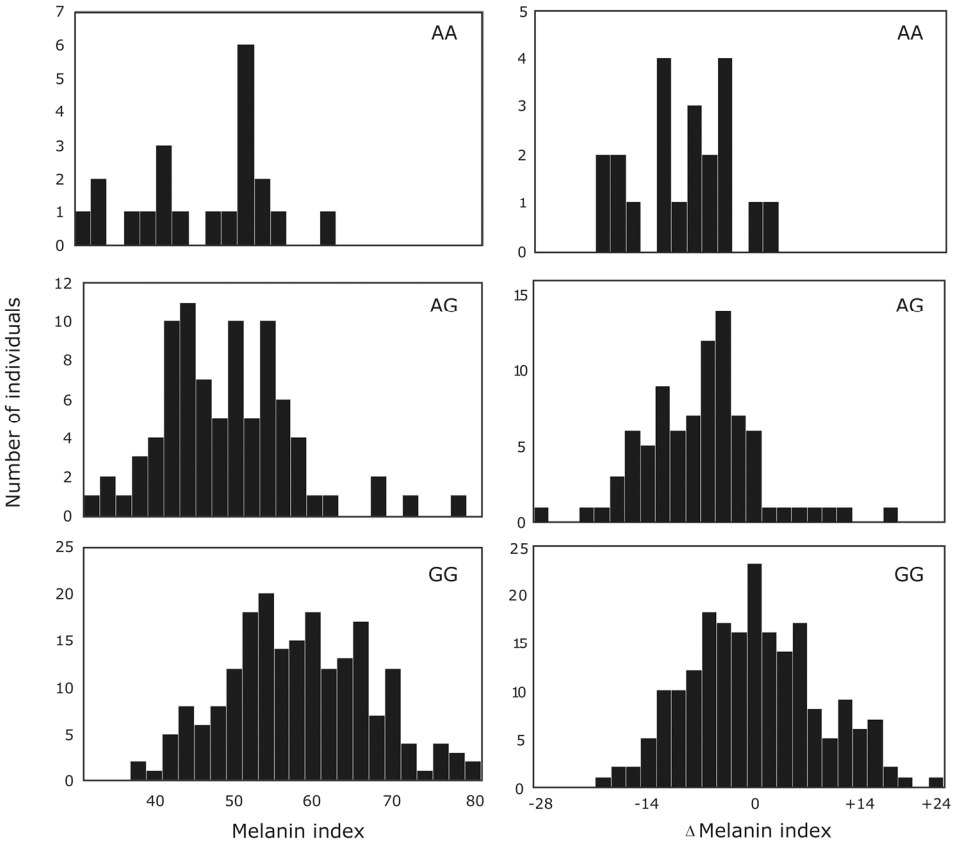

Variation in measured skin pigmentation for each rs1426654 genotype. The left three panels display raw data showing distribution of melanin index in each sub-sample, in which displayed differences reflect both the effect of rs1426654 genotype and the effects of other genes with alleles that correlate with ancestry. The right three panels show the data after adjustment according to regression analysis, as shown in Figure 6B.